AIMS Mathematics, 10(8): 19878–19895.
DOI: 10.3934/math.2025887
Received: 08 July 2025
Revised: 16 August 2025
Accepted: 22 August 2025
Published: 28 August 2025

https://www.aimspress.com/journal/Math

Research article

Dynamical and phenomenological bifurcations induced by multiplicative noise in a stochastic single-species model with double Allee effect

Liang Hong[1] **and Yanhua Yang**[2,*]

[1] College of Mathematics and Statistics, Xinyang Normal University, Xinyang 464000, China
[2] Department of Information Engineering, Xinyang Agriculture and Forestry University, Xinyang 464000, China

* **Correspondence:** Email: xynuhlyyh@xynu.edu.cn.

Abstract: The interplay between system nonlinearity and environmental noise can lead to counterintuitive phenomena that deterministic models are unable to explain. However, the underlying mechanisms are not fully understood. In this study, we proposed a stochastic single-species model driven by multiplicative noise that incorporates a double Allee effect to investigate such counter-intuitive phenomena, specifically dynamical and phenomenological bifurcations induced by noise. Our results underscore the critical role of parameter π, which governs both the persistence and extinction of the species and determines the dynamical and phenomenological bifurcations in the system. Furthermore, our study offers significant biological insights, including: (i) Noise-induced state transitions that alter population density distributions and elevate extinction risk; and (ii) variations in the intensity of the Allee effect, which result in four distinct modifications in the shape of the density function and accelerate the extinction process for endangered species. These findings may have important implications for the management of ecological resources.

Keywords: dynamical and phenomenological bifurcations; stochastic single-species model; double Allee effect; stationary probability density
Mathematics Subject Classification: 34F05, 37H10, 60J70, 92B05

1. Introduction

A key feature of the logistic population model is the gradual decrease in the per capita growth rate as the population abundance increases due to competition for resources. However, some ecosystems show a different pattern at low densities, where the per capita growth rate increases with the population size [1–3]. This phenomenon, known as the Allee effect, is named after ecologist W. C. Allee [4]. In a strong Allee effect, the per capita growth rate can become negative, while in a weak Allee effect, the per

capita growth rate remains positive, albeit at a low level. The Allee effect has significant implications in ecology and evolution [5], especially in population dynamics [6, 7]. For example, Cammarota [8] proposed a modified multi-species competition model that incorporates the mortality-related Allee effect to explore species coexistence. Li and Otto [9] studied traveling waves in a reaction-diffusion model with a strong Allee effect. Rao and Kang [10] investigated a predator-prey reaction-diffusion model with an Allee effect in prey, showing the role of the strength of the Allee effect in shaping distinct spatial patterns. Zeng and Yu [11] established four predator-prey systems with the Allee effect, concluding that these models exhibit more complex dynamical behaviors.

Various mechanisms contributing to the Allee effect have been identified, including but not limited to difficulties in mate finding, reduced anti-predator defense, and inhibition of inbreeding [3]. A simple mathematical form to describe the Allee effect from a single mechanism is through a multiplicative Allee factor, i.e.,

$$\frac{\mathrm{d}x}{\mathrm{d}t} = rx(1 - \frac{x}{K})(x - m), \tag{1.1}$$

where $x = x(t)$ is the population density, K denotes the environmental carrying capacity, and r is the intrinsic growth rate. When $0 < m \ll K$, model (1.1) characterizes a strong Allee effect, as the per capita growth rate becomes negative if the initial population size falls below m. Conversely, when $-K < m < 0$, the model describes a weak Allee effect, where the per capita growth rate remains positive. More importantly, as noted by the authors of [3], two or more mechanisms can simultaneously contribute to the Allee effect within the same population, generating multiple Allee effects. For example, Urocyon littoralis, an endangered species native to California's six Channel Islands, faces threats from predation by Aquila chrysaetos and low reproduction rates in low-density environments due to mate limitation [12]. Consequently, the growth of Urocyon littoralis populations is influenced by the Allee effect arising from both predation pressure and reproductive challenges, resulting in a double Allee effect. To include this phenomenon, Boukal et al. [13] proposed the following single-species model:

$$\frac{\mathrm{d}x}{\mathrm{d}t} = \frac{rx}{x + n}(1 - \frac{x}{K})(x - m) \triangleq xp(x), \tag{1.2}$$

where the function $p(x) = \frac{r}{x+n}(1 - \frac{x}{K})(x - m)$ represents the per capita growth rate, and the auxiliary parameter $n > 0$ quantifies the strength of the Allee effect [14], with $m > -n$. The term $x-m$ is the Allee effect discussed in model (1.1), while the term $\frac{rx}{x+n}$ represents another one caused by external difficulties such as a non-fertile population [15]. So far, various population dynamic models with the double Allee effect have been well studied. Pal and Saha [16] proposed a ratio-dependent prey-predator system by incorporating this effect in prey growth, analyzing its stability and bifurcation dynamics. Later, Jiao and Chen [17] modified this model by introducing predator digestion delay and performed Bogdanov-Takens bifurcation analysis. Singh et al. [18] investigated a modified Leslie-Gower model where the double Allee effect influences the prey population. Xiao and Xia [19] explored Turing instability and bifurcation behaviors in a diffusive predator-prey model with multiple Allee effects and herd behavior.

Research on the impact of stochasticity on population dynamics has attracted increasing attention, especially in conjunction with the Allee effect (for example, [20, 21] and references therein). While noise is often linked to system disorder [22–25], studies show that its interaction with system nonlinearity can produce counter-intuitive phenomena such as stochastic resonance, noise-enhanced stability, and pattern formation [26, 27]. These phenomena play a constructive role in various systems. Stochastic bifurcation, a noise-induced phenomenon, is widely observed and applied across fields [28].

For example, stochastic bifurcation explains patterns in animal behavior in biology [29] and is a useful tool for analyzing market price fluctuations in economics [30]. There are two main types: dynamical bifurcation (D-bifurcation) and phenomenological bifurcation (P-bifurcation) [31]. D-bifurcation focuses on new invariant measures derived from reference measures, particularly the system's stationary probability density [32]. P-bifurcation examines how invariant measures change shape as parameters vary [33]. Moreover, studying stochastic bifurcation is more complex and remains in its early stages both theoretically and methodologically compared to deterministic bifurcation.

Based on the aforementioned analysis, we need to pay more attention to stochastic bifurcation dynamics in population models with the double Allee effect. Despite conducted, unresolved issues remain. First, most researchers have primarily considered environmental noise and the single Allee effect [20, 21], with rarely an attention given to the double Allee effect. Second, researchers have mostly focused on the persistence and extinction of species and the existence of stationary distributions in systems [22,23], with limited attention given to bifurcation dynamics [34–36]. Motivated by this, we investigate the bifurcation dynamics of a stochastic single-species model with the double Allee effect. Our results highlight the role of parameter π, which not only governs the persistence and extinction of species but also determines D-bifurcation and P-bifurcation in the system. Furthermore, our study offers significant biological insights, including: (i) Noise-induced state transitions that alter population density distributions and increase the risk of extinction; and (ii) variations in the strength of the Allee effect that result in four distinct modifications to the shape of the density function, accelerating the extinction process for endangered species. These findings have potential implications for ecological resource management.

The paper is structured as follows: In Section 2, we present the model construction and major findings. In Section 3, we provide proofs of these findings. In Section 4, we provide numerical results to examine the impact of noise and the Allee effect. In Section 5, we conclude with an emphasis on the approach's broad applicability and potential for extending to other models.

2. Model description and main results

2.1. Model description

May [37] pointed out that due to the unpredictability of factors such as rainfall, light intensity, and nutrient availability, parameters in population dynamics are not constants but should exhibit a certain degree of randomness. Theoretically, all parameters (including r and K) in model (1.2) may be subject to random fluctuations, but from a mathematical calculation perspective, this assumption is unrealistic and meaningless in practical applications. In this paper, we assume that environmental noise mainly affects the per capita growth rate, which is also a common practice in the literature [38, 39]. Therefore, $p(x)$ in model (1.2) can be expressed as an average growth rate with a noise term. In cases where the correlation time is short, the noise can be approximated by white noise $\sigma\epsilon(t)$, where $\epsilon(t)$ is standard white noise and σ denotes the noise intensity. Thus, we have

$$\frac{1}{x}\frac{\mathrm{d}x}{\mathrm{d}t} = p(x) + \sigma\epsilon(t). \tag{2.1}$$

Since the accumulated noise up to time t is given by σW_t, where $W_t = \int_0^t \epsilon(\tau)\mathrm{d}\tau$ is a standard Wiener process, Eq (2.1) can be rewritten in the following standard form:

$$\mathrm{d}x = \frac{rx}{x+n}(1-\frac{x}{K})(x-m)\mathrm{d}t + \sigma x \mathrm{d}W_t. \tag{2.2}$$

Our main purpose is to study bifurcation dynamics of stochastic model (2.2) and explore how the double Allee effect influences it. Without loss of generality, assuming $-\frac{nK}{n+K} < m < 0$, we focus only on the weak Allee effect in model (2.2), using a similar approach for the strong Allee effect.

2.2. Main results

One of our goals is to investigate the D-bifurcation of model (2.2) in fluctuating environments. Let

$$\pi = \frac{mr}{n} + \frac{\sigma^2}{2}.$$

We then derive the following inferences about the extinction and persistence of species for stochastic model (2.2).

Theorem 2.1. *(i) If $\pi > 0$, the trivial solution exhibits stochastic asymptotic stability.*

(ii) If $\pi < 0$, model (2.2) *has a unique stationary distribution, where the density function is*

$$\rho(x) = \frac{x^{-\frac{2\pi}{\sigma^2}-1}(x+n)^{\frac{2r}{\sigma^2}(1+\frac{m+n}{K}+\frac{m}{n})}e^{-\frac{2r}{\sigma^2 K}x}}{\int_0^\infty \theta^{-\frac{2\pi}{\sigma^2}-1}(\theta+n)^{\frac{2r}{\sigma^2}(1+\frac{m+n}{K}+\frac{m}{n})}e^{-\frac{2r}{\sigma^2 K}\theta}\mathrm{d}\theta}. \tag{2.3}$$

Remark 2.1. *Theorem 2.1 shows that when $\pi > 0$, model* (2.2) *has a unique stable invariant measure, the Dirac measure δ^* concentrated at 0. When $\pi < 0$, this stability is lost, and a new stable invariant measure appears. Thus, model* (2.2) *undergoes a D-bifurcation as π crosses 0. Consequently, we can draw the following conclusion.*

Theorem 2.2. *Parameter $\pi = 0$ is the D-bifurcation point of model* (2.2).

The following result can be further obtained at the D-bifurcation point.

Theorem 2.3. *If $\pi = 0$, then $\lim_{t\to\infty} x(t) = 0$ in probability.*

Remark 2.2. *Theorems 2.1 and 2.3 show that parameter π determines population survival: Extinction occurs for $\pi \geq 0$, and persistence for $\pi < 0$. Thus, π is the critical threshold that distinguishes population extinction and persistence. Ecologically, parameter π reflects that population survival is determined not only by its intrinsic growth rate and the intensity of the Allee effect, but more critically, by its capacity to withstand the detrimental impacts of environmental stochasticity.*

Another goal of ours is to investigate the P-bifurcation of model (2.2). Since P-bifurcation characterizes changes in the shape of invariant measures under varying parameters, analyzing the extreme points of $\rho(x)$ is essential. A maximum point of $\rho(x)$ suggests that sample trajectories are more likely to concentrate around this point, thereby reflecting stability in probability. Conversely, a minimum point of $\rho(x)$ indicates instability.

From $\frac{\mathrm{d}\rho(x)}{\mathrm{d}x} = 0$, we know that

$$x^{-\frac{2\pi}{\sigma^2}-2}(x+n)^{\frac{2r}{\sigma^2}(1+\frac{m+n}{K}+\frac{m}{n})-1}(d_1x^2+d_2x+d_3) = 0, \tag{2.4}$$

with $d_1 = -\frac{2r}{\sigma^2 K}$, $d_2 = \frac{2r}{\sigma^2}(1+\frac{m}{K})-2$, $d_3 = -n(\frac{2\pi}{\sigma^2}+1)$. Then, Eq (2.4) may possess either a zero root or a maximum two positive roots, as listed in Table 1.

Table 1. Positive roots of Eq (2.4) and shapes of $\rho(x)$.

Parameter		Positive root	Shape of $\rho(x)$
$\pi < -\frac{1}{2}\sigma^2$		1	A peak
$\pi > -\frac{1}{2}\sigma^2$	$d_2 - 2\sqrt{d_1 d_3} > 0$	2	A peak and a valley
	$d_2 - 2\sqrt{d_1 d_3} < 0$	0	Monotonous

Based on the expression of $\rho(x)$ and the distribution of extreme points presented in Table 1, we conclude:

(i) If $\pi < -\sigma^2$, Eq (2.4) has a zero root and a positive root, making $\rho(x)$ unimodal with a peak. It reaches its minimum at $x = 0$ and is differentiable there.

(ii) If $-\sigma^2 < \pi < -\frac{1}{2}\sigma^2$, $\rho(x)$ has a similar shape as in (i) but is not differentiable at $x = 0$.

(iii) If $-\frac{1}{2}\sigma^2 < \pi < 0$, Eq (2.4) has either no roots or two positive roots, making $\rho(x)$ either monotonic or unimodal with a peak and a valley. Additionally, $\lim\limits_{x\to+\infty}\rho(x) = 0$ and $\lim\limits_{x\to 0^+}\rho(x) = +\infty$.

The above analysis shows that as parameter π crosses the thresholds of $-\sigma^2$ and $-\frac{1}{2}\sigma^2$, the shape of $\rho(x)$ transitions from unimodal to one with a peak and valley, and finally to monotonic. Therefore, we reach the following conclusion.

Theorem 2.4. *Stochastic model* (2.2) *exhibits P-bifurcations when parameter* π *crosses* $-\sigma^2$ *and* $-\frac{1}{2}\sigma^2$.

Remark 2.3. *When parameter* π *crosses zero,* $\rho(x)$ *transitions from a Dirac delta function to a power law function, indicating a significant change in the shape of the density function. In a broader context, it can be said that stochastic model* (2.2) *exhibits a P-bifurcation at this critical point.*

3. Proofs of main results

We now provide supplementary findings and proofs for the major results in Section 2.2.

3.1. Preliminaries

Let $C_{\mathbf{b}}^{k,\delta}(\mathbb{R}_+)$ denote the space of continuous functions $f(x)$ from $\mathbb{R}_+$ to $\mathbb{R}$ satisfying $\| f \|_{k,\delta} < \infty$ for any $k \in \mathbb{Z}_+$ and $0 < \delta \leq 1$. Here,

$$\| f \|_{k,0} = \sup_{x\in\mathbb{R}_+}\frac{|f(x)|}{1+|x|} + \sum_{1\leq l\leq k}\sup_{x\in\mathbb{R}_+}|\mathrm{d}^l f(x)|,$$

$$\| f \|_{k,\delta} = \| f \|_{k,0} + \sum_{l=k}\sup_{x\neq y}\frac{|\mathrm{d}^l f(x) - \mathrm{d}^l f(y)|}{|x-y|^\delta}.$$

Consider the Stratonovich stochastic differential equation,

$$\mathrm{d}x(t) = f(x)\mathrm{d}t + g(x) \circ \mathrm{d}W_t, \tag{3.1}$$

where the initial value is given x_0, and $f(x) \in C_{\mathbf{b}}^{1,\delta}(\mathbb{R}_+)$, $g(x) \in C_{\mathbf{b}}^{2,\delta}(\mathbb{R}_+)$ and $\frac{1}{2}g(x)g'(x) \in C_{\mathbf{b}}^{1,\delta}(\mathbb{R}_+)$. Then, we present the following results regarding this equation.

Lemma 3.1. *[40] For the Stratonovich stochastic differential equation* (3.1)*, there exists a unique continuous random dynamical system (RDS)* (θ, φ) *over the metric dynamical system* θ *associated with the Wiener process* W_t *such that* $x(t, \omega) = \varphi(t, \omega)x_0$ *represents a solution to* (3.1) *with a given initial value* x_0*.*

Let $\mathfrak{m}(\mathrm{d}x)$ represent the speed measure on $\mathbb{R}_+$, defined as

$$\mathfrak{m}(A) = \int_A \frac{e^{2\int_1^x \frac{f(\xi)}{g^2(\xi)}\mathrm{d}\xi}}{|g(x)|}\mathrm{d}x, \ A \in \mathfrak{B}(\mathbb{R}_+), \tag{3.2}$$

where $\mathfrak{B}(\mathbb{R}_+)$ represents the Borel σ-algebra of sets in $\mathbb{R}_+$.

Lemma 3.2. *[40] Let* $\mathcal{A}(\omega)$ *denote the random attractor in the universe D consisting of all tempered subsets of* $\mathbb{R}_+$ *for the RDS generated by* (3.1)*. We assume that the following conditions are satisfied:*

(a1) $f(0) = 0$ *and* $f(x) \le k_1 x + k_2$*, where* $k_1, k_2 \in \mathbb{R}_+$*;*

(a2) $g(0) = 0$ *and* $|g'(0)| > 0$*;*

(a3) $\limsup_{x\to\infty} \frac{f(x)}{x} < 0$ *and* $\frac{|g(x)|}{x} = \kappa + O(x^{-\gamma})$*, where both* κ *and* γ *are positive constants.*

Then, we can conclude the following:

(b1) *If* $\mathfrak{m}(0, 1] = \infty$*,* $\mathcal{A}(\omega) = \{0\}$ *almost surely;*

(b2) *If* $\mathfrak{m}(0, 1] < \infty$*, there exists a* $\mathcal{F}$*-measurable equilibrium* $u(\omega)$ *such that* $\mathcal{A}(\omega) = [0, u(\omega)]$ *with* $u(\omega) > 0$ *almost surely. Moreover, there is no other* $\mathcal{F}$*-measurable equilibrium in the set* $(0, u(\omega)]$ *and*

$$\lim_{t\to\infty} \mathbb{P}\{\omega : \varphi(t, \omega)x \in A\} = \mathbb{P}\{\omega : u(\omega) \in A\} = \frac{\mathfrak{m}(A)}{\mathfrak{m}(\mathbb{R}_+)}, \tag{3.3}$$

for all $x > 0$ *and* $A \in \mathfrak{B}(\mathbb{R}_+)$*.*

Lemma 3.3. *[41] Consider the following Itô stochastic differential equation:*

$$\mathrm{d}x(t) = \eta(x)\mathrm{d}t + \mathrm{d}W_t, \tag{3.4}$$

where $\eta(x)$ *is continuously differentiable. If the scale functions*

$$\Psi(y) = \int_0^y e^{\int_0^v 2\eta(\xi)\mathrm{d}\xi}\mathrm{d}v \text{ and } \Phi(y) = \int_0^y e^{-\int_0^v 2\eta(\xi)\mathrm{d}\xi}\mathrm{d}v$$

satisfy $\Psi(-\infty) = -\infty, \Psi(\infty) < \infty, \Phi(-\infty) = -\infty$ *and* $\Phi(+\infty) = +\infty$*, then* $\lim_{t\to+\infty} x(t) = -\infty$ *in probability.*

By employing the established method proposed by Zou et al. [32], the following outcome can be achieved.

Lemma 3.4. *For any initial value* $x_0 \in \mathbb{R}_+$*, model* (2.2) *exhibits a unique solution* $x(t) \in \mathbb{R}_+$ *for all* $t \ge 0$ *almost surely.*

3.2. Proof of Theorem 2.1

Stochastic model (2.2) can be transformed into the following Stratonovich form of equivalent nature:

$$\mathrm{d}x = [\frac{rx}{x+n}(1-\frac{x}{K})(x-m) - \frac{1}{2}\sigma^2 x]\mathrm{d}t + \sigma x \circ \mathrm{d}W_t. \tag{3.5}$$

Denote

$$f(x) = \frac{rx}{x+n}(1-\frac{x}{K})(x-m) - \frac{1}{2}\sigma^2 x,\ g(x) = \sigma x.$$

For the stochastic system (3.5), Lemma 3.1 guarantees the existence of a unique RDS. We further compute that

$$\begin{aligned}\phi(x) \triangleq & e^{2\int_1^x \frac{f(\theta)}{g^2(\theta)}\mathrm{d}\theta}\\ =& e^{2\int_1^x \frac{\frac{r\theta}{\theta+n}(1-\frac{\theta}{K})(\theta-m)-\frac{1}{2}\sigma^2\theta}{\sigma^2\theta^2}\mathrm{d}\theta}\\ =& e^{\frac{2}{\sigma^2}\int_1^x[-(\frac{mr}{n}+\frac{\sigma^2}{2})\frac{1}{\theta}+r(1+\frac{m+n}{K}+\frac{m}{n})\frac{1}{\theta+n}-\frac{r}{K}]\mathrm{d}\theta}\\ =& c_1 x^{-\frac{2\pi}{\sigma^2}}(x+n)^{\frac{2r}{\sigma^2}(1+\frac{m+n}{K}+\frac{m}{n})}e^{-\frac{2r}{\sigma^2 K}x},\end{aligned} \tag{3.6}$$

and here, $c_1 = (1+n)^{-\frac{2r}{\sigma^2}(1+\frac{m+n}{K}+\frac{m}{n})}e^{\frac{2r}{\sigma^2 K}}$. Thus, $\mathfrak{m}(0,1]$ in Lemma 3.2 can be expressed by

$$\begin{aligned}\mathfrak{m}(0,1] =& \int_0^1 \frac{\phi(x)}{\sigma x}\mathrm{d}x\\ =& \frac{c_1}{\sigma}\int_0^1 x^{-\frac{2\pi}{\sigma^2}-1}(x+n)^{\frac{2r}{\sigma^2}(1+\frac{m+n}{K}+\frac{m}{n})}e^{-\frac{2r}{\sigma^2 K}x}\mathrm{d}x.\end{aligned} \tag{3.7}$$

(i) When $\pi > 0$, we have

$$\mathfrak{m}(0,1] \geq \frac{c_1 n^{\frac{2r}{\sigma^2}(1+\frac{m+n}{K}+\frac{m}{n})}e^{-\frac{2r}{\sigma^2 K}}}{\sigma}\int_0^1 x^{-\frac{2\pi}{\sigma^2}-1}\mathrm{d}x = \infty,$$

implying that $\mathcal{A}(\omega) = \{0\}$ almost surely by Lemma 3.2. In other words, the trivial solution is stochastically asymptotically stable.

(ii) When $\pi < 0$, we have

$$\mathfrak{m}(0,1] \leq \frac{c_1(1+n)^{\frac{2r}{\sigma^2}(1+\frac{m+n}{K}+\frac{m}{n})}}{\sigma}\int_0^1 x^{-\frac{2\pi}{\sigma^2}-1}\mathrm{d}x < \infty.$$

Based on Lemma 3.2, system (3.5) exhibits a unique stationary distribution; similarly, model (2.2) also possesses this characteristic.

Denote

$$\rho(x) = \frac{\phi(x)}{g(x)\mathfrak{m}(\mathbb{R}_+)}.$$

It is easy to verify that $\rho(x)$ is the solution of the following Fokker-Planck equation corresponding to model (3.5):

$$\frac{\mathrm{d}}{\mathrm{d}x}[(f(x)+\frac{1}{2}g'(x)g(x))\rho(x)] - \frac{1}{2}\frac{\mathrm{d}^2}{\mathrm{d}x^2}[g^2(x)\rho(x)] = 0.$$

Therefore, $\rho(x)$ can be explicitly expressed as

$$\rho(x) = \frac{x^{-\frac{2\pi}{\sigma^2}-1}(x+n)^{\frac{2r}{\sigma^2}(1+\frac{m+n}{K}+\frac{m}{n})}e^{-\frac{2r}{\sigma^2 K}x}}{\int_0^\infty \theta^{-\frac{2\pi}{\sigma^2}-1}(\theta+n)^{\frac{2r}{\sigma^2}(1+\frac{m+n}{K}+\frac{m}{n})}e^{-\frac{2r}{\sigma^2 K}\theta}\mathrm{d}\theta}.$$

3.3. Proof of Theorem 2.3

Let $\varpi(t) = \frac{\ln x(t)}{\sigma}$. Applying Itô's formula to $\varpi(t)$, we obtain $\mathrm{d}\varpi(t) = \eta(\varpi)\mathrm{d}t + \mathrm{d}W_t$, where

$$\eta(\varpi) = \frac{1}{\sigma}[\frac{r}{e^{\sigma\varpi}+n}(1-\frac{e^{\sigma\varpi}}{K})(e^{\sigma\varpi}-m) - \frac{\sigma^2}{2}].$$

After basic algebraic calculations,

$$\begin{aligned}
\int_0^v 2\eta(\theta)\mathrm{d}\theta =& \frac{2}{\sigma}\int_0^v [\frac{r}{e^{\sigma\theta}+n}(1-\frac{e^{\sigma\theta}}{K})(e^{\sigma\theta}-m) - \frac{\sigma^2}{2}]\mathrm{d}\theta \\
=& \frac{2}{\sigma^2}\int_1^{e^{\sigma v}} [-(\frac{mr}{n}+\frac{\sigma^2}{2})\frac{1}{\xi} + r(1+\frac{m+n}{K}+\frac{m}{n})\frac{1}{\xi+n} - \frac{r}{K}]\mathrm{d}\xi \\
=& \frac{2}{\sigma^2}[-(\frac{mr}{n}+\frac{\sigma^2}{2})\sigma v + r(1+\frac{m+n}{K}+\frac{m}{n})\ln(e^{\sigma v}+n) - \frac{r}{K}e^{\sigma v}] + c_2 \\
=& \frac{2}{\sigma^2}[r(1+\frac{m+n}{K}+\frac{m}{n})\ln(e^{\sigma v}+n) - \frac{r}{K}e^{\sigma v}] + c_2,
\end{aligned}$$

and here, $c_2 = -r(1+\frac{m+n}{K}+\frac{m}{n})\ln(1+n) + \frac{r}{K}$. Consequently, $\Psi(y)$ defined in Lemma 3.3 can be expresses as

$$\begin{aligned}
\Psi(y) =& \int_0^y e^{\int_0^v 2\eta(\theta)\mathrm{d}\theta}\mathrm{d}v \\
=& \int_0^y e^{\frac{2}{\sigma^2}[r(1+\frac{m+n}{K}+\frac{m}{n})\ln(e^{\sigma v}+n) - \frac{r}{K}e^{\sigma v}] + c_2}\mathrm{d}v \\
=& e^{c_2}\int_0^y (e^{\sigma v}+n)^{\frac{2r}{\sigma^2}(1+\frac{m+n}{K}+\frac{m}{n})} e^{-\frac{2r}{\sigma^2 K}e^{\sigma v}}\mathrm{d}v \\
=& \frac{e^{c_2}}{\sigma}\int_1^{e^{\sigma y}} \frac{(\xi+n)^{\frac{2r}{\sigma^2}(1+\frac{m+n}{K}+\frac{m}{n})} e^{-\frac{2r}{\sigma^2 K}\xi}}{\xi}\mathrm{d}\xi.
\end{aligned}$$

Due to $\lim\limits_{y\to-\infty} e^{\sigma y} = 0$ and $\lim\limits_{y\to+\infty} e^{\sigma y} = +\infty$,

$$\begin{aligned}
\Psi(-\infty) =& -\frac{e^{c_2}}{\sigma}\int_0^1 \frac{(\xi+n)^{\frac{2r}{\sigma^2}(1+\frac{m+n}{K}+\frac{m}{n})} e^{-\frac{2r}{\sigma^2 K}\xi}}{\xi}\mathrm{d}\xi \\
\le& -\frac{e^{c_2}}{\sigma}\int_0^1 \frac{n^{\frac{2r}{\sigma^2}(1+\frac{m+n}{K}+\frac{m}{n})} e^{-\frac{2r}{\sigma^2 K}}}{\xi}\mathrm{d}\xi \\
=& -\frac{n^{\frac{2r}{\sigma^2}(1+\frac{m+n}{K}+\frac{m}{n})} e^{c_2-\frac{2r}{\sigma^2 K}}}{\sigma}\int_0^1 \frac{1}{\xi}\mathrm{d}\xi = -\infty,
\end{aligned}$$

and

$$\Psi(+\infty) = \frac{e^{c_2}}{\sigma}\int_1^{+\infty} \frac{(\xi+n)^{\frac{2r}{\sigma^2}(1+\frac{m+n}{K}+\frac{m}{n})} e^{-\frac{2r}{\sigma^2 K}\xi}}{\xi}\mathrm{d}\xi.$$

To prove the boundedness of $\Psi(+\infty)$, we split the integration interval $[1,+\infty)$ into two sub-intervals: $[1,\max 1,n]$ and $[\max 1,n,+\infty)$. Then,

$$\Psi(+\infty) = \frac{e^{c_2}}{\sigma}\int_1^{\max\{1,n\}} \frac{(\xi+n)^{\frac{2r}{\sigma^2}(1+\frac{m+n}{K}+\frac{m}{n})} e^{-\frac{2r}{\sigma^2 K}\xi}}{\xi}\mathrm{d}\xi + \frac{e^{c_2}}{\sigma}\int_{\max\{1,n\}}^{+\infty} \frac{(\xi+n)^{\frac{2r}{\sigma^2}(1+\frac{m+n}{K}+\frac{m}{n})} e^{-\frac{2r}{\sigma^2 K}\xi}}{\xi}\mathrm{d}\xi.$$

By the continuity of

$$\frac{(\xi+n)^{\frac{2r}{\sigma^2}(1+\frac{m+n}{K}+\frac{m}{n})}e^{-\frac{2r}{\sigma^2 K}\xi}}{\xi}$$

on $[1, \max\{1, n\}]$, there exists a positive constant K_1 such that

$$\frac{e^{c_2}}{\sigma}\int_1^{\max\{1,n\}}\frac{(\xi+n)^{\frac{2r}{\sigma^2}(1+\frac{m+n}{K}+\frac{m}{n})}e^{-\frac{2r}{\sigma^2 K}\xi}}{\xi}\mathrm{d}\xi \le K_1.$$

Furthermore,

$$\begin{aligned}
&\frac{e^{c_2}}{\sigma}\int_{\max\{1,n\}}^{+\infty}\frac{(\xi+n)^{\frac{2r}{\sigma^2}(1+\frac{m+n}{K}+\frac{m}{n})}e^{-\frac{2r}{\sigma^2 K}\xi}}{\xi}\mathrm{d}\xi\\
&\le \frac{e^{c_2}}{\sigma}\int_{\max\{1,n\}}^{+\infty}\frac{(2\xi)^{\frac{2r}{\sigma^2}(1+\frac{m+n}{K}+\frac{m}{n})}e^{-\frac{2r}{\sigma^2 K}\xi}}{\xi}\mathrm{d}\xi\\
&= \frac{e^{c_2}}{\sigma}\Big(\frac{\sigma^2 K}{r}\Big)^{\frac{2r}{\sigma^2}(1+\frac{m+n}{K}+\frac{m}{n})}\int_{\frac{2r\max\{1,n\}}{\sigma^2 K}}^{+\infty} t^{\frac{2r}{\sigma^2}(1+\frac{m+n}{K}+\frac{m}{n})-1}e^{-t}\mathrm{d}t\\
&\le \frac{e^{c_2}}{\sigma}\Big(\frac{\sigma^2 K}{r}\Big)^{\frac{2r}{\sigma^2}(1+\frac{m+n}{K}+\frac{m}{n})}\Gamma\Big(\frac{2r}{\sigma^2}\Big(1+\frac{m+n}{K}+\frac{m}{n}\Big)\Big) \triangleq K_2,
\end{aligned}$$

where $\Gamma(\cdot)$ is the Gamma function. Then, we have

$$\Psi(+\infty) \le K_1 + K_2 < +\infty.$$

Furthermore, $\Phi(-\infty) = -\infty$ and $\Phi(+\infty) = +\infty$ can be obtained similarly. Therefore, $\lim_{t\to\infty} x(t) = 0$ in probability by Lemma 3.3.

4. Numerical results

Numerical simulations are performed in this section to validate the theoretical findings and explore the impact of environmental noise for the stochastic model (2.2).

4.1. The impact of noise intensity on survival and D-bifurcation

Let $r = 1$, $n = 2$, $m = -1$, and $K = 10$. If $\sigma = 1.5$, we have $\pi = \frac{mr}{n} + \frac{\sigma^2}{2} = 0.63 > 0$. According to Theorem 2.1, the population tends to extinction, as shown in Figure 1(a1). If $\sigma = 1$, one has $\pi = 0$, which also results in population extinction; see Figure 1(b1). Both scenarios exhibit a unique stable invariant measure concentrated at 0, as observed from Figures 1(a2) and (b2). However, when selecting $\sigma = 0.5$, we find that $\pi = -0.38 < 0$. In this case, the population persists with a nontrivial stationary distribution, illustrated in Figures 1(c1) and (c2). From an ecological perspective, parameter π governs both persistence and extinction of the population and acts as a D-bifurcation point.

When considering a smaller noise level of $\sigma = 0.1$ that satisfies $\pi = -0.5$, sample paths exhibit minor oscillations around the deterministic attractor, as illustrated in Figures 1(d1) and (d2). By comparing the various subgraphs in Figure 1, it can be observed that lower-level noise has minimal impact on the original dynamics, while higher-level noise lead to population extinction regardless of the persistence in the deterministic system. This phenomenon is further elucidated in Figure 2.

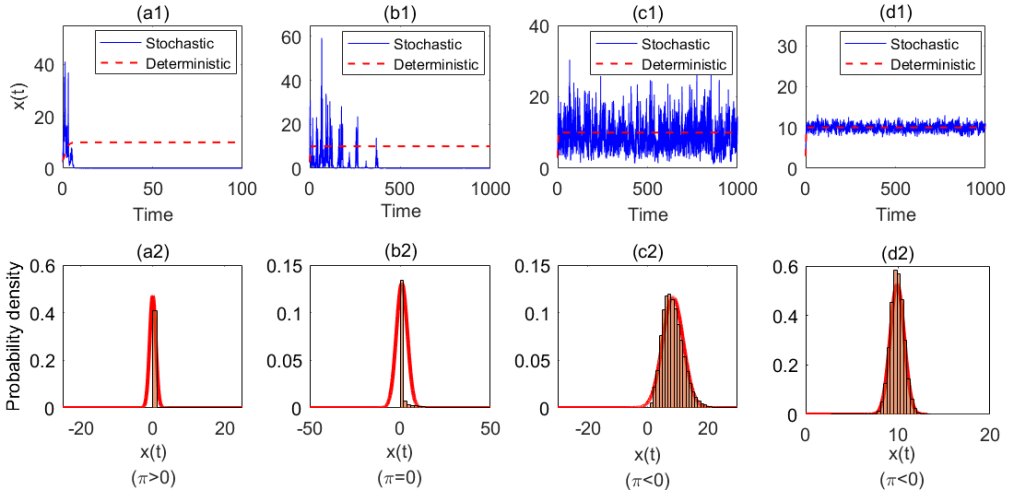

Figure 1. The upper half-plane shows the trajectories of stochastic model (2.2) and its deterministic counterpart under different noise intensities σ. Specifically, (a1) $\sigma = 1.5$ satisfies $\pi = 0.63 > 0$, (b1) $\sigma = 1$ satisfies $\pi = 0$, (c1) $\sigma = 0.5$ satisfies $\pi = -0.38 < 0$, and (d1) $\sigma = 0.1$ satisfies $\pi = -0.5 < 0$. The lower half-plane displays the corresponding histograms.

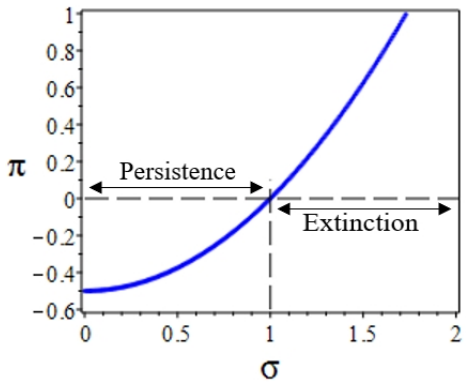

Figure 2. The relationship between the critical threshold π and the noise intensity σ.

4.2. The impact of noise intensity on P-bifurcation

Let $n = 2$, $m = -1$, and $K = 10$. Figure 3 shows a bifurcation diagram in the $\sigma^2 - r$ plane, illustrating how noise intensity affects bifurcation dynamics. We note that the plane is divided into five zones by the following curves:

$$L_1 : \pi = 0;\ L_2 : \pi = -\frac{\sigma^2}{2};\ L_3 : \pi = -\sigma^2;\ L_4 : d_2 - 2\sqrt{d_1 d_3} = 0.$$

Here, zone ① indicates the extinction of the population , while zones ②–⑤ indicate the persistence of the population. Specifically, in zone ②, the density function $\rho(x)$ exhibits monotonic behavior, while in zone ③, it exhibits a unimodal structure with both a peak and a valley. Moreover, zones ④ and ⑤ display a unimodal structure for the density function but only with a peak. Notably, the density function

is not differentiable at $x = 0$ in zone ④ but is differentiable in zone ⑤. Therefore, the system undergoes four P-bifurcations as noise intensity changes.

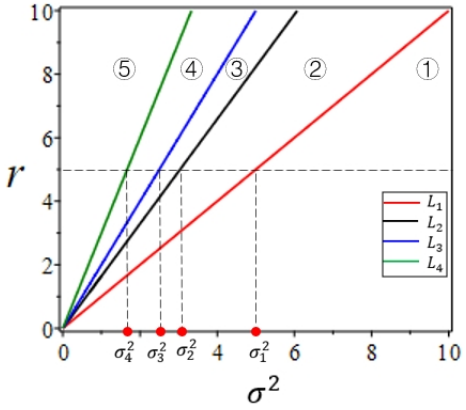

Figure 3. The bifurcation diagram of model (2.2) shows that the $\sigma^2 - r$ plane is divided into five distinct zones. There is no nontrivial stationary distribution in zone ①, while it exists in zones ②–⑤. In zone ②, the density function $\rho(x)$ exhibits monotonic behavior. In contrast, zones ③, ④, and ⑤ exhibit a unimodal structure with distinct characteristics: Zone ③ features both a peak and a valley, whereas zones ④ and ⑤ exhibit only a peak. Notably, the density function is non-differentiable at $x = 0$ in zone ④ but is differentiable in zone ⑤.

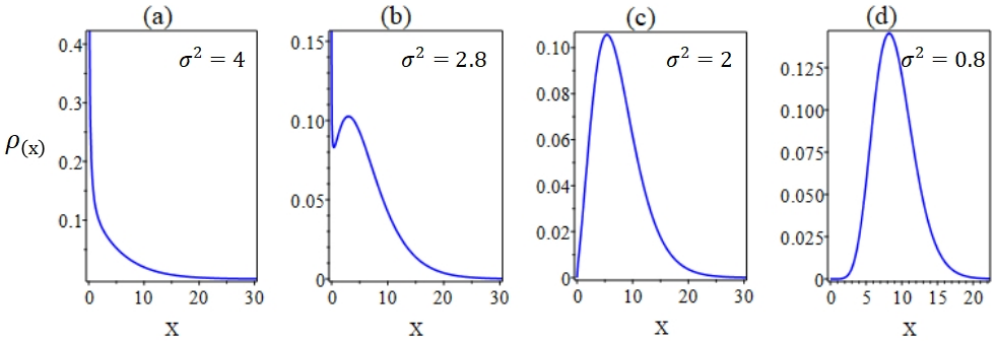

Figure 4. The graph illustrates different structures of the density function $\rho(x)$ under different noise intensities σ: (a) monotonous structure; (b) unimodal structure with a peak and a valley; (c) unimodal structure with only a peak, non-differentiable at $x = 0$; and (d) unimodal structure with only a peak, differentiable at $x = 0$.

To demonstrate bifurcation dynamics more intuitively, we present numerical results with $r = 5$. Here, the critical noise levels are $\sigma_1^2 = 5$, $\sigma_2^2 = 3.04$, $\sigma_3^2 = 2.5$, and $\sigma_4^2 = 1.67$. For any noise intensity satisfying $\sigma^2 > 5$, the population tends toward extinction, resulting in the absence of a nontrivial stationary distribution. Sample paths for this case are similar to Figure 1(a1) and thus omitted. When $\sigma = 2$ (i.e., $3.04 < \sigma^2 < 5$), the density function shows monotonic behavior, as shown in Figure 4(a). Upon decreasing the noise intensity to $\sqrt{2.8}$ (i.e., $2.5 < \sigma^2 < 3.04$), a unimodal density function characterized by both a peak and a valley emerges (see Figure 4(b)). Notably, in both cases, it can be observed that $\lim_{x\to+\infty} \rho(x) = 0$ and $\lim_{x\to 0^+} \rho(x) = +\infty$. Moreover, further reducing the noise intensity to $\sqrt{2}$

(i.e., $1.67 < \sigma^2 < 2.5$) results in a unimodal density function with only a peak and is not differentiable at $x = 0$ (see Figure 4(c)). Finally, setting $\sigma = \sqrt{0.8}$ (i.e., $\sigma^2 < 1.67$) yields a density function similar to Figure 4(c) but it is differentiable at $x = 0$ (see Figure 4(d)).

In summary, as noise intensity decreases, the density function undergoes four P-bifurcations. From an ecological standpoint, noise can induce state transitions within the system, thereby altering population density distributions and increasing the risk of population extinction. This conclusion is also supported by Figure 5, which visually demonstrates the effects of varying noise intensity for both the extreme points and peak values of the density function $\rho(x)$.

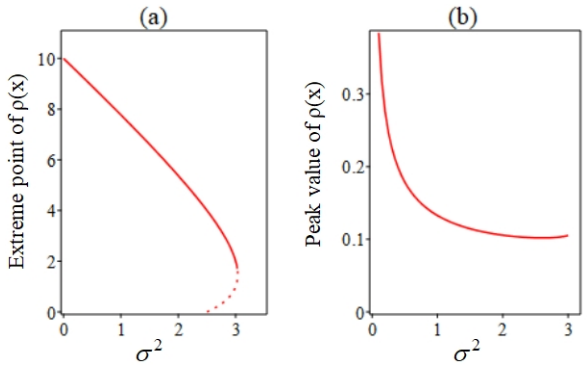

Figure 5. (a) The relationship between the extreme points (solid line for maximum, dashed line for minimum) of $\rho(x)$, and the noise intensity σ is shown; and (b) the relationship between the peak values of $\rho(x)$, and the noise intensity σ is illustrated.

4.3. The impact of Allee effect on stochastic dynamics

Considering the auxiliary parameter n as a quantification of the intensity of the Allee effect, we set $r = 1$, $m = -1$, $K = 10$, $\sigma = 0.5$, and enable variations in n to examine its impact on stochastic dynamics. Initially, we plot the relationship between the critical threshold π and the auxiliary parameter, with n plotted first, as depicted in Figure 6. Evidently, this graph vividly demonstrates that a stronger Allee effect has an adverse impact on population sustainability.

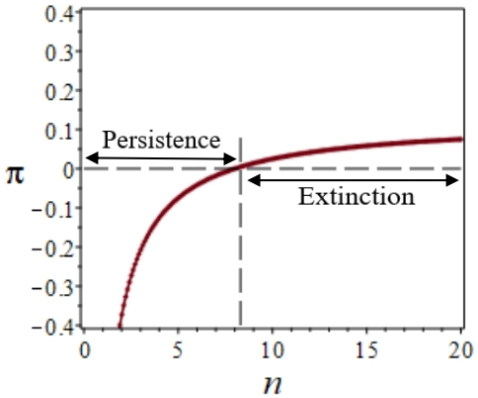

Figure 6. The relationship between the critical threshold π and auxiliary parameter n.

The impact of auxiliary parameter n on both the extreme points and peak values of $\rho(x)$ is shown in Figure 7. It can be observed that as n gradually increases, $\rho(x)$ transitions from exhibiting a single

maximum point to displaying both maximum and minimum points before vanishing. Furthermore, its peak value decreases progressively. To further clarify this behavior, we present the graph of $\rho(x)$ under varying values of n, as shown in Figure 8. As the auxiliary parameter values decrease, the shape structure of the density function undergoes four distinct changes. By comparing Figure 4 with 8, it is evident that both the Allee effect and noise intensity have analogous impacts, resulting in four characteristic changes in the shape of the density function, namely four P-bifurcations.

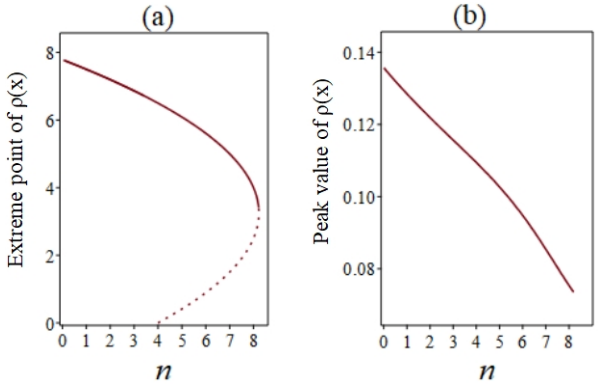

Figure 7. (a) The relationship between the extreme points (solid line for maximum and dashed line for minimum) of $\rho(x)$, and the auxiliary parameter n is shown; and (b) the relationship between the peak values of $\rho(x)$, and the auxiliary parameter n is illustrated.

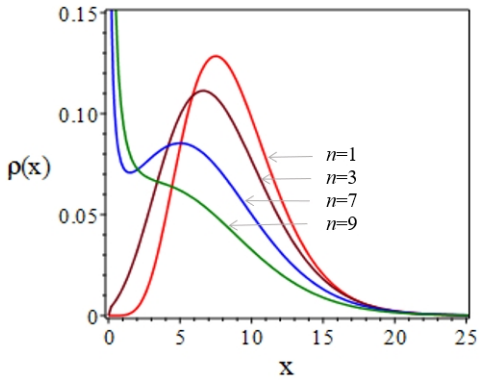

Figure 8. The graph shows different structures of the density function $\rho(x)$ under different auxiliary parameters n. The red line represents a unimodal structure with a peak that is differentiable at $x = 0$. The dark red depicts a unimodal structure with a peak that is not differentiable at $x = 0$. The blue line illustrates a unimodal structure characterized by both a peak and a valley. The green line exhibits a monotonic structure.

5. Discussion

Our focus of this paper lies in examining the bifurcation dynamics observed in a stochastic single-species model featuring a double Allee effect driven by multiplicative noise. Theoretical and numerical results demonstrate that the original dynamic behavior remains largely unaffected by lower-level noise, whereas higher-level noise induces population extinction regardless of its persistence in its

corresponding deterministic system. Interestingly, moderate level noise may induce diverse alterations in the system state. Our results underscore the critical role of parameter π, which governs both the persistence and extinction of species and determines the dynamical and phenomenological bifurcations in the system. Furthermore, our study offers significant biological insights, including: (i) Noise-induced state transitions that alter population density distributions and increase the risk of extinction; and (ii) variations in the strength of the Allee effect that result in four distinct modifications to the shape of the density function, accelerating the extinction process for endangered species.

The exploitation of biological resources and the harvesting of species are commonly employed strategies for economic purposes. However, implementing effective harvest management policies can safeguard populations facing extinction due to excessive harvesting [42, 43]. Let the harvesting function of the population be denoted as $h(x)$. Consequently, when subjected to harvesting, stochastic model (2.2) can be formulated as follows:

$$\mathrm{d}x = [\frac{rx}{x+n}(1-\frac{x}{K})(x-m) - h(x)]\mathrm{d}t + \sigma x \mathrm{d}W_t. \tag{5.1}$$

It is important to mention that the function $h(x)$ can be expressed in various forms, such as constant harvesting, linear harvesting, and non-linear harvesting [44, 45]. For simplicity, we illustrate the universality of the method used in this paper by taking only nonlinear harvesting (Michaelis-Menten type harvesting) as an example, i.e.,

$$h(x) = \frac{ax}{b+x}, \tag{5.2}$$

with both a and b as positive constants. Then, $f(x)$ and $g(x)$ in Eq (3.1) becomes

$$f(x) = x[\frac{r}{x+n}(1-\frac{x}{K})(x-m) - \frac{a}{b+x} - \frac{1}{2}\sigma^2],\ g(x) = \sigma x.$$

Denote

$$\pi = \frac{mr}{n} + \frac{a}{b} + \frac{\sigma^2}{2}.$$

Further calculations show that $\phi(x)$ in Eq (3.6) is given by

$$\begin{aligned}
\phi(x) \triangleq & e^{2\int_1^x \frac{f(\theta)}{g^2(\theta)}\mathrm{d}\theta} \\
= & e^{2\int_1^x \frac{\frac{r}{\theta+n}(1-\frac{\theta}{K})(\theta-m)-\frac{a}{b+\theta}-\frac{1}{2}\sigma^2}{\sigma^2\theta}\mathrm{d}\theta} \\
= & e^{\frac{2}{\sigma^2}\int_1^x[-(\frac{mr}{n}+\frac{a}{b}+\frac{\sigma^2}{2})\frac{1}{\theta}+r(1+\frac{m+n}{K}+\frac{m}{n})\frac{1}{\theta+n}+\frac{a}{b(\theta+b)}-\frac{r}{K}]\mathrm{d}\theta} \\
= & c_1 x^{-\frac{2\pi}{\sigma^2}}(x+n)^{\frac{2r}{\sigma^2}(1+\frac{m+n}{K}+\frac{m}{n})}(x+b)^{\frac{2a}{\sigma^2 b}}e^{-\frac{2r}{\sigma^2 K}x},
\end{aligned} \tag{5.3}$$

and here, $c_1 = (1+n)^{-\frac{2r}{\sigma^2}(1+\frac{m+n}{K}+\frac{m}{n})}(1+b)^{-\frac{2a}{\sigma^2 b}}e^{\frac{2r}{\sigma^2 K}}$. Subsequently, by following the approach employed in the proofs of Theorems 2.1 and 2.3, we deduce that, for stochastic model (5.1) with (5.2),

(i) if $\pi \geq 0$, the population $x(t)$ will become extinct;

(ii) if $\pi < 0$, stochastic model (5.1) possesses a unique stationary distribution with the density function given by

$$\rho(x) = \frac{x^{-\frac{2\pi}{\sigma^2}-1}(x+n)^{\frac{2r}{\sigma^2}(1+\frac{m+n}{K}+\frac{m}{n})}(x+b)^{\frac{2a}{\sigma^2 b}}e^{-\frac{2r}{\sigma^2 K}x}}{\int_0^\infty \theta^{-\frac{2\pi}{\sigma^2}-1}(\theta+n)^{\frac{2r}{\sigma^2}(1+\frac{m+n}{K}+\frac{m}{n})}(\theta+b)^{\frac{2a}{\sigma^2 b}}e^{-\frac{2r}{\sigma^2 K}\theta}\mathrm{d}\theta}.$$

On the other hand, D-bifurcation and P-bifurcation can be discussed similarly. Therefore, the method adopted in this article has broad applicability and can be extended to other models.

In this paper, we investigate has investigated the combined effects of noise and the Allee effect on bifurcation dynamics within a stochastic single-species model incorporating multiplicative noise. The results may have important implications for the management of ecological resources; however, several unresolved issues remain, warranting further research. For instance, researchers could focus on deriving the probability density function and analyzing bifurcation behavior in more realistic, high-dimensional systems.

Author contributions

Liang Hong: Writing–original draft, Methodology, Formal analysis, Software; Yanhua Yang: Conceptualization, Writing–review & editing, Funding acquisition. All authors have read and approved the final version of the manuscript for publication.

Use of Generative-AI tools declaration

The authors declare they have not used Artificial Intelligence (AI) tools in the creation of this article.

Acknowledgments

The work was supported by the Key Scientific Research Project of Colleges and Universities of Henan Province (No. 24A110012).

Conflict of interest

The authors declare that they have no known competing financial interests or personal relationships that could have appeared to influence the work reported in this paper.

References

1. F. Courchamp, L. Berec, J. Gascoigne, *Allee effects in ecology and conservation*, Oxford University Press, 2008.
2. J. C. Gascoigne, R. N. Lipcius, Allee effects driven by predation, *J. Appl. Ecol.*, **41** (2004), 801–810. https://doi.org/10.1111/j.0021-8901.2004.00944.x
3. L. Berec, E. Angulo, F. Courchamp, Multiple Allee effects and population management, *Trends Ecol. Evol.*, **22** (2007), 185–191. https://doi.org/10.1016/j.tree.2006.12.002
4. W. C. Allee, *Animal aggregations: a study in general sociology*, Chicago: The University of Chicago Press, 1931. https://doi.org/10.5962/bhl.title.7313
5. A. M. Kramer, L. Berec, J. M. Drake, Editorial: Allee effects in ecology and evolution, *J. Anim. Ecol.*, **87** (2018), 7–10. https://doi.org/10.1111/1365-2656.12777

6. J. S. Cánovas, M. Muñoz-Guillermo, On a population model with density dependence and Allee efect, *Theory Biosci.*, **142** (2023), 423–441. https://doi.org/10.1007/s12064-023-00407-y
7. D. Senc, S. Ghorai, M. Banerjee, A. Morozov, Bifurcation analysis of the predator-prey model with the Allee effect in the predator, *J. Math. Biol.*, **84** (2022), 7. https://doi.org/10.1007/s00285-021-01707-x
8. D. Cammarota, N. Z. Monteiro, R. Menezes, H. Fort, A. M. Segura, Lotka-Volterra model with Allee effect: equilibria, coexistence and size scaling of maximum and minimum abundance, *J. Math. Biol.*, **87** (2023), 82. https://doi.org/10.1007/s00285-023-02012-5
9. B. T. Li, G. Otto, Forced traveling waves in a reaction-diffusion equation with strong Allee effect and shifting habitat, *Bull. Math. Biol.*, **85** (2023), 121. https://doi.org/10.1007/s11538-023-01221-9
10. F. Rao, Y. Kang, The complex dynamics of a diffusive prey-predator model with an Allee effect in prey, *Ecol. Complexity*, **28** (2016), 123–144. https://doi.org/10.1016/j.ecocom.2016.07.001
11. Y. N. Zeng, P. Yu, Complex dynamics of predator-prey systems with Allee effect, *Int. J. Bifur. Chaos*, **32** (2022), 2250203. https://doi.org/10.1142/S0218127422502030
12. E. Angulo, G. W. Roemer, L. Berec, J. Gascoigne, F. Courchamp, Double Allee effects and extinction in the island fox, *Conserv. Biol.*, **21** (2007), 1082–1091. https://doi.org/10.1111/j.1523-1739.2007.00721.x
13. D. S. Boukal, M. W. Sabelis, L. Berec, How predator functional responses and Allee effects in prey affect the paradox of enrichment and population collapses, *Theoret. Popul. Biol.*, **72** (2007), 136–147. https://doi.org/10.1016/j.tpb.2006.12.003
14. X. S. Li, D. F. Pang, P. Wallhead, R. G. J. Bellerby, Dynamics of an aquatic diffusive predator-prey model with double Allee effect and *pH*-dependent capture rate, *Chaos Solitons Fract.*, **169** (2023), 113234. https://doi.org/10.1016/j.chaos.2023.113234
15. H. Barclay, M. Mackauer, The sterile insect release method for pest control: a density-dependent model, *Environ. Entomol.*, **9** (1980), 810–817. https://doi.org/10.1093/ee/9.6.810
16. P. J. Pal, T. Saha, Qualitative analysis of a predator-prey system with double Allee effect in prey, *Chaos Solitons Fract.*, **73** (2015), 36–63. https://doi.org/10.1016/j.chaos.2014.12.007
17. J. F. Jiao, C. Chen, Bogdanov-Takens bifurcation analysis of a delayed predator-prey system with double Allee effect, *Nonlinear Dyn.*, **104** (2021), 1697–1707. https://doi.org/10.1007/s11071-021-06338-x
18. M. K. Singh, B. S. Bhadauria, B. K. Singh, Bifurcation analysis of modified Leslie-Gower predator-prey model with double Allee effect, *Ain Shams Eng. J.*, **9** (2018), 1263–1277. https://doi.org/10.1016/j.asej.2016.07.007
19. J. L. Xiao, Y. H. Xia, Spatiotemporal dynamics in a diffusive predator-prey model with multiple Allee effect and herd behavior, *J. Math. Anal. Appl.*, **529** (2024), 127569. https://doi.org/10.1016/j.jmaa.2023.127569
20. I. Bashkirtseva, L. Ryashko, B. Spagnolo, Combined impacts of the Allee effect, delay and stochasticity: persistence analysis, *Commun. Nonlinear Sci. Numer. Simul.*, **84** (2020), 105148. https://doi.org/10.1016/j.cnsns.2019.105148

21. M. D. Asfaw, S. M. Kassa, E. M. Lungu, Stochastic plant-herbivore interaction model with Allee effect, *J. Math. Biol.*, **79** (2019), 2183–2209. https://doi.org/10.1007/s00285-019-01425-5
22. A. Sau, B. Saha, S. Bhattacharya, An extended stochastic Allee model with harvesting and the risk of extinction of the herring population, *J. Theor. Biol.*, **503** (2020), 110375. https://doi.org/10.1016/j.jtbi.2020.110375
23. B. Q. Zhou, D. Q. Jiang, T. Hayat, Analysis of a stochastic population model with mean-reverting Ornstein-Uhlenbeck process and Allee effects, *Commun. Nonlinear Sci. Numer. Simul.*, **111** (2022), 106450. https://doi.org/10.1016/j.cnsns.2022.106450
24. X. W. Yu, Y. L. Ma, An avian influenza model with nonlinear incidence and recovery rates in deterministic and stochastic environments, *Nonlinear Dyn.*, **108** (2022), 4611–4628. https://doi.org/10.1007/s11071-022-07422-6
25. X. W. Yu, Y. L. Ma, Complex dynamics of a dysentery diarrhoea epidemic model with treatment and sanitation under environmental stochasticity: persistence, extinction and ergodicity, *IEEE Access*, **9** (2021), 161129–161140. https://doi.org/10.1109/ACCESS.2021.3132386
26. F. Borgogno, P. D'Odorico, F. Laio, L. Ridolfi, Stochastic resonance and coherence resonance in groundwater-dependent plant ecosystems, *J. Theor. Biol.*, **293** (2012), 65–73. https://doi.org/10.1016/j.jtbi.2011.09.015
27. C. H. Zeng, C. Zhang, J. K. Zeng, H. C. Luo, D. Tian, H. L. Zhang, et al., Noises-induced regime shifts and -enhanced stability under a model of lake approaching eutrophication, *Ecol. Complexity*, **22** (2015), 102–108. https://doi.org/10.1016/j.ecocom.2015.02.005
28. C. L. Luo, S. J. Guo, Stability and bifurcation of two-dimensional stochastic differential equations with multiplicative excitations, *Bull. Malays. Math. Sci. Soc.*, **40** (2017), 795–817. https://doi.org/10.1007/s40840-016-0313-7
29. R. Mankin, T. Laas, A. Sauga, A. Ainsaa, E. Reiter, Colored-noise-induced Hopf bifurcations in predator-prey communities, *Phys. Rev. E*, **74** (2006), 021101. https://doi.org/10.1103/PhysRevE.74.021101
30. C. Chiarella, X. Z. He, D. Wang, M. Zheng, The stochastic bifurcation behavior of speculative financial markets, *Phys. A*, **387** (2008), 3837–3846. https://doi.org/10.1016/j.physa.2008.01.078
31. L. Arnold, N. S. Namachchivaya, K. R. Schenk-Hoppé, Toward an understanding of stochastic Hopf bifurcation: a case study, *Int. J. Bifur. Chaos*, **6** (1996), 1947–1975. https://doi.org/10.1142/S0218127496001272
32. X. L. Zou, Y. T. Zheng, L. R. Zhang, J. L. Lv, Survivability and stochastic bifurcations for a stochastic Holling type II predator-prey model, *Commun. Nonlinear Sci. Numer. Simul.*, **83** (2020), 105136. https://doi.org/10.1016/j.cnsns.2019.105136
33. N. S. Namachchivaya, Stochastic bifurcation, *Appl. Math. Comput.*, **38** (1990), 101–159. https://doi.org/10.1016/0096-3003(90)90051-4
34. Y. Zhu, L. Wang, Z. P. Qiu, Threshold dynamics of a stochastic single population model with Allee effect, *Appl. Math. Lett.*, **143** (2023), 108689. https://doi.org/10.1016/j.aml.2023.108689
35. C. Q. Xu, Effects of colored noises on the statistical properties of a population growth model with Allee effect, *Phys. Scr.*, **95** (2020), 075215. https://doi.org/10.1088/1402-4896/ab93a8

36. X. W. Yu, Y. L. Ma, Noise-induced dynamics in a single species model with Allee effect driven by correlated colored noises, *J. Theor. Biol.*, **573** (2023), 111610. https://doi.org/10.1016/j.jtbi.2023.111610

37. R. M. May, P. M. Allen, Stability and complexity in model ecosystems, *IEEE Trans. Syst. Man Cybernet.*, **SMC-6** (2001), 887. https://doi.org/10.1109/TSMC.1976.4309488

38. C. Carlos, C. A. Braumann, General population growth models with Allee effects in a random environment, *Ecol. Complexity*, **30** (2017), 26–33. https://doi.org/10.1016/j.ecocom.2016.09.003

39. A. Potapov, H. Rajakaruna, Allee threshold and stochasticity in biological invasions: colonization time at low propagule pressure, *J. Theor. Biol.*, **337** (2013), 1–14. https://doi.org/10.1016/j.jtbi.2013.07.031

40. I. Chueshov, *Monotone random systems theory and applications*, Berlin, Heidelberg: Springer, 2002. https://doi.org/10.1007/b83277

41. D. L. Zhao, S. L. Yuan, Critical result on the break-even concentration in a single-species stochastic chemostat model, *J. Math. Anal. Appl.*, **434** (2016), 1336–1345. https://doi.org/10.1016/j.jmaa.2015.09.070

42. G. R. Munro, Mathematical bioeconomics and the evolution of modern fisheries economics, *Bull. Math. Biol.*, **54** (1992), 163–184.

43. M. M. Chen, R. Yuan, Maximum principle for the optimal harvesting problem of a size-stage-structured population model, *Discrete Contin. Dyn. Syst. B*, **27** (2022), 4619–4648. https://doi.org/10.3934/dcdsb.2021245

44. X. Y. Meng, J. Li, Dynamical behavior of a delayed prey-predator-scavenger system with fear effect and linear harvesting, *Int. J. Biomath.*, **14** (2021), 2150024. https://doi.org/10.1142/S1793524521500248

45. S. K. Mandal, D. K. Jana, S. Poria, The role of harvesting in population control in the presence of correlated noise sources, *Phys. Scr.*, **97** (2022), 065006. https://doi.org/10.1088/1402-4896/ac6f91

AIMS Press

© 2025 the Author(s), licensee AIMS Press. This is an open access article distributed under the terms of the Creative Commons Attribution License (https://creativecommons.org/licenses/by/4.0)